Localization in chaotic systems with a single-channel opening

Domenico Lippolis,[1,2,*] Jung-Wan Ryu,[2,3] and Sang Wook Kim[4]
[1]*Institute for Advanced Study, Tsinghua University, Beijing 100084, China*
[2]*Department of Physics, Pusan National University, Busan 609-735, South Korea*
[3]*School of Electronics Engineering, Kyungpook National University, Daegu 702-701, South Korea*
[4]*Department of Physics Education, Pusan National University, Busan 609-735, South Korea*
(Received 23 August 2014; revised manuscript received 1 June 2015; published 30 July 2015)

We introduce a single-channel opening in a random Hamiltonian and a quantized chaotic map: localization on the opening occurs as a sensible deviation of the wave-function statistics from the predictions of random matrix theory, even in the semiclassical limit. Increasing the coupling to the open channel in the quantum model, we observe a similar picture to resonance trapping, made of a few fast-decaying states, whose left (right) eigenfunctions are entirely localized on the (preimage of the) opening, and plentiful long-lived states, whose probability density is instead suppressed at the opening. For the latter, we derive and test a linear relation between the wave-function intensities and the decay rates, similar to the Breit-Wigner law. We then analyze the statistics of the eigenfunctions of the corresponding (discretized) classical propagator, finding a similar behavior to the quantum system only in the weak-coupling regime.

DOI: 10.1103/PhysRevE.92.012921 PACS number(s): 05.45.Mt, 03.65.Ta, 05.70.Ln, 89.70.Cf

I. INTRODUCTION

One of the distinctive traits of all chaotic systems is their seemingly "random" behavior [1]. As a consequence, one usually assumes that the eigenfunctions of a quantized chaotic Hamiltonian have the same statistical properties (i.e., wave-function intensity distribution) of a complete set of waves with random amplitudes and phases [2,3], or equivalently, of the eigenvectors of a Hermitian matrix with random entries, according to random matrix theory (RMT) [4,5]. Due to a number of applications (quantum information theory [6–8], classical [9,10] and quantum optics [11–13], quantum transport [14,15], etc.), as well as to equally many theoretical issues (see, for example, [16–18]), the quantum chaos community is largely focused at present on the behavior of *open* systems [19].

In this paper, we address one of the simplest theoretical questions, namely whether and how the wave-function statistics deviates from the predictions of the random wave assumption as we perturb a chaotic system with a single-channel opening. As the main result of our investigation, we found numerically that the overall wave-function intensity distribution at the location of the opening does change from the RMT-expected χ^2 shape to a longer-tailed curve, which is analytically described using perturbation theory. Physically, this implies that localization occurs at the opening. In our theory, the opening can be an arbitrary state $|a\rangle$ in the Hilbert space; however, in most of our testing models we take it as a coherent state in the phase space.

Deviations of the wave-function statistics from RMT have been observed before in real space: for time-reversal-symmetric systems, it was conjectured [20] and then shown analytically and experimentally [21] that the distribution of the wave functions at the leads smoothly crosses over from Porter-Thomas to Poisson distribution with the coupling to the opening. Although there was no explicit mention of localization, the wave-function distribution for a two-channel opening was found to be an inverse square root, of much slower decay than the RMT prediction. In a later work [22], this behavior was related to the correlations between real and imaginary parts of the wave function, which may depend in general on the underlying classical dynamics.

On the other hand, real- and phase-space localization have been detected in closed systems in correspondence with the so-called scars [23,24]. Within that framework, the distribution of the intensities on an unstable periodic orbit was found to decay more slowly than the RMT-expected distribution [25], due to the phenomenon of constructive interference. This is not our case: in order to rule out scarring, we place our probe states away from periodic orbits. Still, the localization found for weak coupling to the opening does hold in the semiclassical limit, which makes us think of a classical effect.

Successively, we follow the evolution of the wave-function statistics of the quantum map for strong coupling to the opening. As a result, the intensity distribution becomes separated into several long-lived- and a few short-lived eigenstates. We show that their intensities are proportional to their decay rates, arguing that this quantum effect can be explained with the existing theories on resonance trapping [26,27]. In particular, the intensities of the long-lived states depend on the escape rates through a linear relation akin to the Breit-Wigner law [3].

In the second part of the paper, we perform analogous simulations on the classical cat map, and, by looking at the statistics of the eigenfunctions of the classical propagator (Perron-Frobenius operator [28]), we find the deviation from the closed system to be similar to the quantum case for weak coupling to the opening. This observation corroborates the hypothesis of a classical mechanism behind localization in this regime. On the contrary, we show that a strongly coupled opening does not result in resonance trapping, which makes the classical setting substantially different from the quantum setting in this regime.

The paper is organized as follows: In Sec. II A we calculate the deviation of the wave-function statistics from

*domenico@tsinghua.edu.cn

an exponential distribution due to a single-channel opening by using first-order perturbation theory. In Sec. II B we verify the theoretical expectation using random Hamiltonians drawn from the Gaussian unitary ensemble (GUE) [5], and successively on the eigenfunctions of the quantized cat map [29]. Section II C deals with the strong-coupling regime: we analyze the proportionality between escape rates and intensities, while we account for the localization patterns of left and right fastest-decaying eigenfunctions in Sec. II D. In Sec. III we introduce the Perron-Frobenius operator of the same test map as a classical propagator, and we demonstrate numerically an analogous deviation from RMT of its eigenfunction statistics for both weak and strong couplings to a small opening in the phase space. A summary and conclusions are given in Sec. IV.

II. WAVE-FUNCTION INTENSITY DISTRIBUTION

A. Theory

Suppose H_0 is a GUE Hamiltonian. Since its eigenfunctions are complex valued, their intensities $x = |\langle a|\psi_0\rangle|^2$ at a certain state $|a\rangle$ follow the exponential distribution [3]

$$P(x) = e^{-x}. \tag{1}$$

Now we open the system at $|a\rangle$ [18],

$$H = H_0 - i\frac{\Gamma}{2}|a\rangle\langle a|, \tag{2}$$

and ask how the distribution of intensities $z = |\langle a|\psi\rangle|^2$ is changed with respect to the exponential, when Γ is small enough. By using perturbation theory [30–33], we expand the amplitudes $\langle a|\psi\rangle$ in first order as

$$\langle a|\psi_n\rangle \simeq \langle a|\psi_n^0\rangle - i\Gamma\langle a|\psi_n^0\rangle \sum_{p\neq n} \frac{|\langle\psi_p^0|a\rangle|^2}{2(E_n - E_p)}. \tag{3}$$

Left and right eigenfunctions are generally distinct for the non-Hermitian operator (2), but they are just the complex conjugate of each other in the first-order perturbation regime. We recognize two uncorrelated quantities: $\xi \equiv \langle a|\psi_n^0\rangle$, whose real and imaginary parts are Gaussian distributed, and $\eta \equiv \sum_{p\neq n} \frac{|\langle\psi_p^0|a\rangle|^2}{2(E_n - E_p)}$, following

$$P_1(\eta) \propto \left(\frac{1}{1+\gamma^2\eta^2}\right)^2 \tag{4}$$

with $\gamma = \Delta E\pi^{-1}$, and ΔE the average level spacing of H_0 (see the derivation in Appendix and [30]). We seek the distribution of the variable $z \equiv |\langle a|\psi\rangle|^2 = \xi^2 + \Gamma^2\xi^2\eta^2$, namely

$$P(z) = \int d\xi\, d\eta\, \delta(z - \xi^2 - \Gamma^2\xi^2\eta^2) P_0(\xi) P_1(\eta)$$
$$= \frac{2\gamma}{\pi} \int \frac{d\eta\, e^{-z/(1+\Gamma^2\eta^2)}}{(1+\gamma^2\eta^2)^2(1+\Gamma^2\eta^2)}, \tag{5}$$

where $P_0(\xi) \propto e^{-\xi^2}$. We immediately see that its expectation value

$$\langle z\rangle = \frac{\Gamma^2 + \gamma^2}{\gamma^2} \tag{6}$$

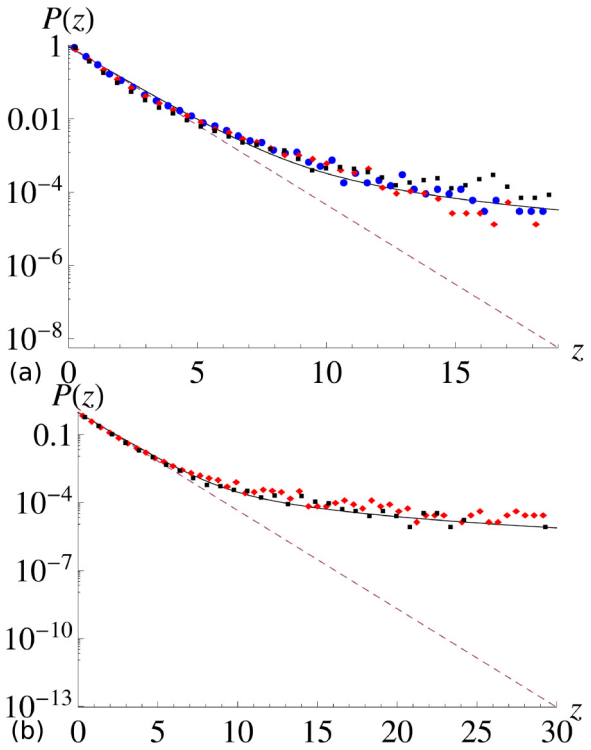

FIG. 1. (Color online) (a) Rescaled sample distributions of the overall wave-function intensities $P(z = |\langle a|\psi\rangle|^2)$ in a logarithmic scale, obtained diagonalizing several realizations of a GUE Hamiltonian, for $N = 16\,384$ (dots, 8 realizations), $N = 4096$ (diamonds, 18 realizations), $N = 200$ (squares, 600 realizations), and loss parameter $\Gamma = 0.5$; solid and dashed lines are the theoretical expectation (5) and the exponential distribution (1), respectively. (b) The same analysis with the quantum cat map (14): $N = 4096$ (diamonds, 28 realizations), $N = 200$ (squares, 600 realizations), and $\Gamma = 1$.

always exceeds unity, meaning the opening produces a longer tail than the exponential distribution (1) we started with, and therefore a certain amount of localization of the probability density occurs.

B. Numerical tests

We now verify the theoretical intensity distribution (5) first by diagonalizing multiple realizations of the non-Hermitian Hamiltonian (2), where both H_0 and the amplitudes $\langle a|\psi_n^0\rangle$ are drawn from the Gaussian unitary ensemble (GUE). The resulting probability distribution for the wave-function intensities $|\langle a|\psi\rangle|^2$ in the first-order perturbation regime agrees with the expression (5) as shown in the example of Fig. 1(a). The dimension of the Hilbert space chosen ranges from $N = 200$ to 16 384, suggesting that the result holds in the semiclassical limit. We will go back to this issue in Sec. III.

Figure 1(b) shows that our prediction for a perturbed GUE Hamiltonian also fits the distribution of the wave-function intensities of the quantized kicked cat map with a small opening. The classical evolution of the cat map reads [29,34]

$$F_\epsilon = F_0 \circ M_\epsilon, \tag{7}$$

with

$$F_0 : \begin{pmatrix} q' \\ p' \end{pmatrix} = \begin{pmatrix} 1 & 1 \\ 1 & 2 \end{pmatrix} \begin{pmatrix} q \\ p \end{pmatrix} \mod 1 \tag{8}$$

and

$$M_\epsilon : \begin{pmatrix} q' \\ p' \end{pmatrix} = \begin{pmatrix} q - \epsilon \sin(2\pi p) \\ p \end{pmatrix} \mod 1. \tag{9}$$

The quantization of the map is given by [29,35]

$$U_\epsilon = U_0 V_\epsilon, \tag{10}$$

where

$$\langle q_j | U_0 | q_k \rangle = N^{-1/2} e^{i\pi/4} e^{2\pi N i (q_j^2 - q_j q_k + q_k^2/2)} \tag{11}$$

and

$$\langle q_j | V_\epsilon | q_k \rangle = \sum_{p_m} \frac{1}{N} e^{Ni(-\epsilon \cos 2\pi p_m + 2\pi (q_j - q_k) p_m)}. \tag{12}$$

The quantization of the linear map (8) is known to possess pseudosymmetries [36] that cause the spectral statistics to deviate from the circular unitary ensemble (CUE), hence the use of the perturbation (9) to restore the RMT behavior. Here the opening is a minimum-uncertainty Gaussian wave packet

$$\langle q | a \rangle = \left(\frac{1}{\pi \hbar^2} \right)^{1/4} e^{-(q-q_0)^2/2\hbar + i p_0 (q - q_0)/\hbar}, \tag{13}$$

whose center (q_0, p_0) is chosen at random on the unit torus (the scar at the origin [34,37] is carefully avoided). The nonunitary propagator is realized by replacing U_ϵ of (10) with [18,37]

$$U = \left(1 - \frac{\Gamma}{2} |a\rangle\langle a| \right) U_\epsilon. \tag{14}$$

All the steps of the derivation of Eq. (5) would still hold in this case, except for Eq. (4), since the quasienergies of the cat map follow the statistics of the CUE instead of the GUE's. Still, both are asymptotically equivalent for $N \to \infty$ [5]. In our simulations, we alternatively set $N = 200$ and 4096, and we produce an ensemble statistics of over 10^5 states by repeatedly diagonalizing the matrix (14) over different values of the kick strength ϵ, chosen at random within the range [0.1,0.2].

C. Strong coupling to the opening

When we further increase the coupling Γ in the propagator (14), the curve (5) no longer fits the numerical data, as we leave the perturbation regime. Few short-lived left eigenstates are localized on the opening, while the rest are characterized by intensity suppression together with small decay rates. We will clarify the localization patterns of left and right eigenfunctions in Sec. II D, while we focus for the moment on the left ones. The overlaps between the open region and the eigenstates are presented as a function of the decay rate in Fig. 2(a), reminiscent of the so-called "resonance trapping" effect [26,27,38–44], whose main results we summarize as follows.

Consider the complex eigenvalues of H, $E_n - i\gamma_n$, γ_n being the decay rates. It has been observed and explained [27,39] that when the overall loss $w = \sum_n \gamma_n$ is greater than the energy range ΔE where the levels are located, there exists one particularly short-lived state $|\psi_1\rangle$, having a decay

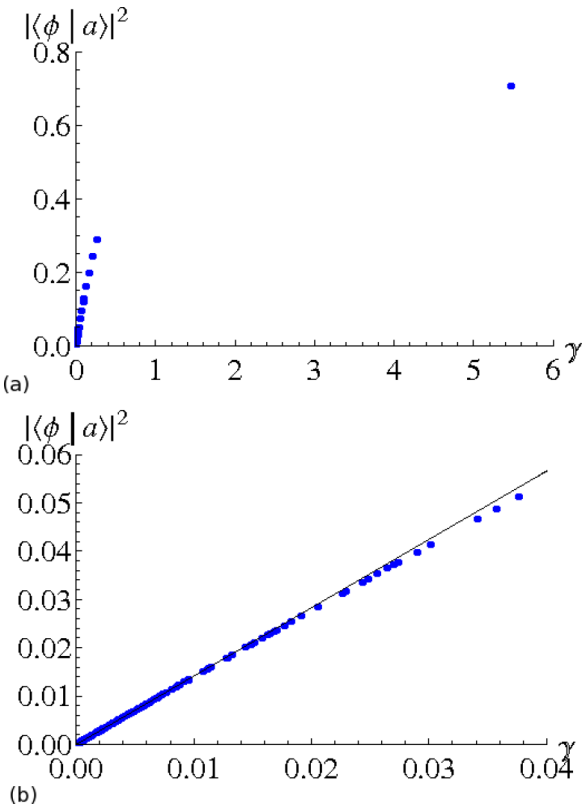

FIG. 2. (Color online) (a) Overlaps between the opening and the left eigenfunctions of the quantized cat map vs decay rates γ, showing the resonance trapping effect. (b) The linear part of the data is well described by Eq. (18); here $\Gamma = 2\sqrt{2}$.

rate $\gamma_1 = w - O(\Delta E/w)$, while the rest of the modes have $\gamma_{n\neq 1} = O(\Delta E/w)$, so that they are "trapped" near the real axis, although still complex-valued. We will now use this property together with a P-Q projection formalism to explain the linear dependence of the intensities $|\langle \phi_{n\neq 1} | a \rangle|^2$ on the decay rates in this regime. Let PHP be the projection of the Hamiltonian onto the fast-decaying state, $P = |\psi_1\rangle\langle\phi_1|$, and let QHQ be the projection on the remaining states, $Q = \sum_{n\neq 1} |\psi_n\rangle\langle\phi_n|$. We first write an eigenvalue of QHQ as

$$\begin{aligned} (E_j - i\gamma_j) &= \langle \phi_j | QHQ | \psi_j \rangle \\ &= \langle \phi_j | Q H_0 Q | \psi_j \rangle - i \frac{\Gamma}{2} \langle \phi_j | Q | a \rangle \langle a | Q | \psi_j \rangle. \end{aligned} \tag{15}$$

On the other hand, we know that QHQ is almost Hermitian, so that, to a very good approximation,

$$(Q|\psi_j\rangle)^\dagger = \langle \phi_j | Q. \tag{16}$$

We can now recognize the eigenvalues as

$$E_j - i\gamma_j \simeq \langle \phi_j | H_0 | \phi_j \rangle - i \frac{\Gamma}{2} |\langle a | \phi_j \rangle|^2, \tag{17}$$

where the first term is the expectation value of a Hermitian operator, hence a real number, and therefore

$$\gamma_j = \frac{\Gamma}{2} |\langle a | \phi_j \rangle|^2, \tag{18}$$

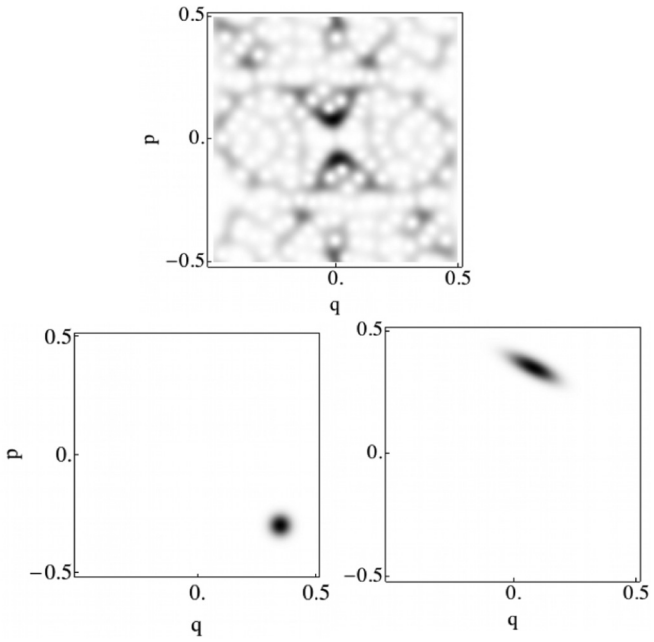

FIG. 3. Husimi distribution of the fastest decaying eigenstate of the quantized cat map. Top: for the closed system; bottom: the left and right eigenfunctions of the same state, for the open map with loss parameter $\Gamma = 2\sqrt{2}$. The opening is placed exactly at the position where the Husimi distribution of the left eigenfunction is localized.

so that we "return" to a Breit-Wigner kind of law, as verified in Fig. 2(b) for the simulations of the cat map.

D. Left and right eigenfunctions

We notice that in the strong-coupling regime, the left and right eigenfunctions of the propagator (14) are well distinct. In particular, we show in Fig. 3 the Husimi distributions of the fastest-decaying eigenstates, whose *left* eigenfunctions only are supported on the opening. This is explained as follows:

The discrete-time evolution operator (14) is indeed split into unitary evolution U_0 and a projection describing the opening, $P_o = 1 - |a\rangle\langle a|$, so that $U = P_o U_0$. Given the eigenvalue λ_j and its eigenfunctions $\langle\phi_j|$ and $|\psi_j\rangle$,

$$\begin{aligned} \langle\phi_j|P_o U_0|x\rangle &= \lambda_j^*\langle\phi_j|x\rangle, \\ \langle x|P_o U_0|\psi_j\rangle &= \lambda_j\langle x|\psi_j\rangle. \end{aligned} \tag{19}$$

The projection P_o acts first on the left eigenfunction, so that in order for the loss to be maximal, the amplitudes $\langle\phi_j|x\rangle$ should be supported on the opening, in our case the coherent state $|a\rangle$. On the other hand, the unitary propagator U_0 acts first on the *right* eigenfunction $|\psi_j\rangle$: in one time step we approximate the quantum evolution with the classical map $F(x)$, and

$$|\langle x|U_0|\psi_j\rangle|^2 \simeq |F[\psi_j(x)]|^2, \tag{20}$$

so that the decay rate is highest if $|\psi_j\rangle$ is supported on the classical *preimage* of the opening, $F^{-1}(o)$ [37,45] (Fig. 3). The localization patterns of left and right eigenfunctions will differ most when they occur where the system is more sensitive to initial conditions, typically away from fixed points or stable/unstable manifolds of the classical map.

In general the outcomes depend on how the propagation and the loss are arranged, which is usually $U = P_o U_0$ as in our model, but they can be inverted sometimes [46].

III. CLASSICAL SYSTEM

In this section, we consider a classical chaotic map with a small opening, again looking for deviations from RMT of the sample distributions of the wave-function intensities, properly defined. The idea is to fit the numerical data with analytic formulas obtained equivalently to (5) in the perturbation regime, and then to extend the analysis to a strongly coupled opening, as is done in the quantum setting.

Using the density operator $\hat\rho$, the wave-function intensities in the quantum regime can be written as

$$|\langle a|\psi\rangle|^2 = \langle a|\hat\rho|a\rangle. \tag{21}$$

Here $\hat\rho$ obeys the Liouville–von Neumann equation [47]

$$i\hbar\partial_t\hat\rho = [H,\hat\rho], \tag{22}$$

whose classical analog is [48]

$$\partial_t\rho = \{H,\rho\}. \tag{23}$$

The classical Liouville propagator can be written as

$$U_{\rm cl}^t = e^{i\hat L t}, \tag{24}$$

where $\hat L = \{H,\cdot\}$ is the Liouville differential operator. In the Hamiltonian case, $\hat L^\dagger = -\hat L$, and therefore the evolution (24) is unitary. The classical evolution operator is supported on a space of generalized functions, and its spectrum has a discrete and a continuous part (Stone's theorem); all the eigenfrequencies lie on the unit circle. In particular, ergodic and mixing systems only have one isolated eigenvalue, $e^{i\omega_0} = 1$, while the rest of the spectrum is continuous [49].

In reality, every system experiences noise, coming, for example, from uncertainties or roundoff errors. However small, noise breaks unitarity and changes the spectrum of the Liouville propagator, from continuous to discrete [50]. The ("leading") unit eigenvalue is still there, but the rest of the spectrum moves inside the unit circle. Because of the noise, the propagator acquires a smooth kernel [51], which makes the eigenfunctions also smooth. In a closed system, the ground-state eigenfunction of an eigenvalue equal to unity (natural measure) is real and positive-definite, the density to which all initial conditions asymptotically converge. The other eigenfunctions are in general complex and called "relaxation modes," as they are associated with the decay of correlations [28]:

$$\langle g|\mathcal{L}|f\rangle = \sum e^{-\gamma_n}\langle g|\rho_n\rangle\langle\tilde\rho_n|f\rangle. \tag{25}$$

The classical-to-quantum correspondence was studied by Fishman and co-workers [52,53], who found that the formal solution to the classical Liouville equation, called the Perron-Frobenius operator [here $x = (q,p)$],

$$(\mathcal{L}^t\circ\rho)(x) = \int_{\mathcal{M}} dx_0\,\delta\big(x - f^t(x_0)\big)\rho(x_0,0), \tag{26}$$

when discretized, effectively behaves like the weakly noisy operator, and it has the same spectrum as the quantum

propagator of the Wigner function in the classical limit (a similar result was shown in [54]).

Based on that, we can say that the noise introduced by the discretization washes out the fine details of the chaotic dynamics, and makes the random-wave assumption hold for the eigenfunctions of (26). These are smooth and complex valued (in the phase space), and therefore their squared magnitudes ("intensities") $|\rho_n(x)|^2$ follow a χ^2 distribution. Ideally, the classical limit of the minimum-uncertainty wave packet would correspond to just one cell of the phase-space discretization. Here we want to repeat the analysis carried in the quantum setting and appreciate the difference in the statistics of the eigenfunctions from the closed to the open system. We believe this is done most effectively by taking the sum of the square magnitudes over a small phase-space interval, as

$$\xi_n = \int_{\mathcal{M}_o} dx_0 \int dx |\rho_n(x)|^2 \delta(x - x_0), \tag{27}$$

which is the overlap of $|\rho_n(x)|^2$ with a δ function [classical limit of the coherent state $|a\rangle$ of Eq. (13)] supported on the probing region $\mathcal{M}_o$. The quantum analog of Eq. (27) would be $\sum_{a'} |\langle a'|\psi\rangle|^2$ over a number of probe states. In that case, the probability density $P(\sum_{a'} |\langle a'|\psi\rangle|^2)$ for the unperturbed system is a χ^2 distribution with M degrees of freedom,

$$P_M(\xi) = \frac{\xi^{M/2-1} e^{-\xi/2}}{\Gamma\left(\frac{1}{2}M\right) 2^{M/2}}, \tag{28}$$

which becomes a Gaussian as $M \to \infty$.

We then perform numerical simulations on the classical cat map (7): the Perron-Frobenius operator is discretized with the Ulam method [55],

$$[\mathcal{L}]_{ij} = \frac{1}{|\mathcal{M}_i|} \int_{\mathcal{M}_i} dx \int_{\mathcal{M}_j} dy\, \delta(y - f(x)). \tag{29}$$

The entries $[\mathcal{L}]_{ij}$ are estimated using a straightforward Monte Carlo technique [56], based on counting how many trajectories starting from each $\mathcal{M}_j$ land in $\mathcal{M}_i$. A partial opening is realized by randomly decreasing the number of trajectories that start from the hole, which overall covers a tiny 1% of the available phase space. The $10^4 \times 10^4$ matrix (29) is then diagonalized. Figure 4(a) shows a fast-decaying eigenfunction peaked in correspondence with the hole, as an extreme case

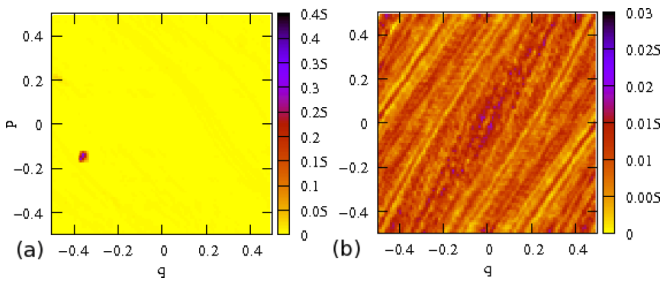

FIG. 4. (Color online) Absolute values of (a) a fast- and (b) a slow-decaying eigenfunction of the evolution operator (26) for the open cat map (7), with the hole located in the square $[-0.4, -0.3] \times [-0.2, -0.1]$, obtained diagonalizing a $10^4 \times 10^4$ discretization (29). The manifold structure of the cat map is shown in (b).

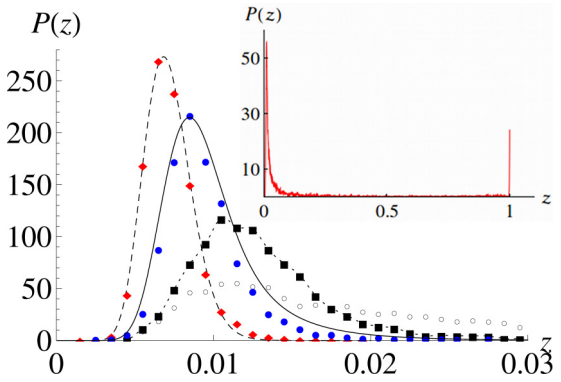

FIG. 5. (Color online) Sample distributions of the intensities ξ [given by Eq. (27)] of the eigenfunctions of the Perron-Frobenius operator for the cat map (7): diamonds, closed system; filled dots, 25% partial opening; squares, 50% partial opening; empty dots, 75% partial opening; dashed curve, Eq. (28) rescaled to the data set, where the number of degrees of freedom has been fitted from the data to $M = 46$; solid curve, Eq. (32) with $M = 46$, while $\tilde{\Gamma} = 1$ is fitted from the data. Inset: full opening at the same location; the peak at the tail is due to the instantaneous-decay states.

of density enhancement at the opening. We then measure the statistics of the intensities (27) in both the closed and open systems (Fig. 5): while the sample taken from the closed system agrees with the law (28) (M is fitted from the data), the "intensities" on the opening exhibit a longer tail, as in the quantum regime. We qualitatively account for this observation by performing the convolution (5) on the unperturbed distribution (28), this time in M degrees of freedom,

$$P(z) \propto \int r^{M-1} dr\, d\eta\, \delta(z - r^2 - \tilde{\Gamma}^2 r^2 \eta^2) e^{-r^2/2} P_M(\eta), \tag{30}$$

where $r^2 = \sum_x |\rho_n(x)|^2$ (here x is discretized by our grid), while the perturbation η follows [30]:

$$P_M(\eta) \propto \left(\frac{1}{1 + \gamma^2 \eta^2}\right)^{1+M/2}. \tag{31}$$

The outcome is

$$P_M(z) = C_M \int d\eta \frac{z^{M/2-1} e^{-z/2(1+\tilde{\Gamma}^2\eta^2)}}{(1 + \tilde{\Gamma}^2\eta^2)^{M/2} (1 + \gamma^2\eta^2)^{1+M/2}}, \tag{32}$$

where $\gamma = \pi^{-1}$, $C_M = \frac{2^{-1-M/2} M}{\pi^{3/2} \Gamma(\frac{1+M}{2})}$, while $\tilde{\Gamma}$ is fitted from the sample distribution. Figure 5 also shows two sample distributions of the intensities obtained for stronger couplings to the opening, away from the perturbation regime: importantly, the trend of a flatter curve with a longer tail stays qualitatively the same, indicating an increasing number of fast-decaying states. A full opening introduces a number of instantaneous-decay states [45] that completely localize on the hole. That generates a peak at the very tail of the sample distribution, whose shape remains otherwise qualitatively the same as for the partial openings (inset of Fig. 5, note the scale). As seen, the quantum system in the same regime behaves differently, as the states that do not decay instantaneously are instead long-lived, and the overall intensity distribution is consistent with the resonance-trapping picture.

We may now give an interpretation of our findings. An open system, be it classical or quantum, must allow for some fast-decaying initial conditions, among the others. Densities and wave functions must be expressible in terms of the eigenstates of the linear operators we are using. As a consequence, some of these eigenstates also decay fast and are more concentrated on the opening and its preimages [45]. For weak coupling, both classical and quantum simulations fit this physical picture, and they behave likewise. Moreover, the calculated deviations of the intensity distributions from the RMT results all rely on perturbation theory, which can be applied to any linear operator with a discrete, nondegenerate spectrum. That is the case for both the quantum Hamiltonian/propagator and the discretized classical evolution operator.

On the other hand, classical and quantum systems behave differently when strongly coupled to the opening, the latter only displaying resonance trapping, while the former does not show any signatures of mode interaction.

IV. SUMMARY

We have shown the following:

(i) The overall wave-function intensity distribution of a random (GUE) Hamiltonian and a quantized chaotic map deviates from the predictions of RMT, when a weakly coupled, single-channel opening is introduced. The result holds in the semiclassical limit.

(ii) By further increasing the coupling to the open channel in our model, few states localize on the opening particularly strongly and decay fast, while the rest show the opposite behavior, i.e., slow decay together with intensity suppression at the opening. Using well-known results in the context of the resonance trapping effect, we derived a linear relation between the intensities of the long-lived states and their decay rates, similar to the Breit-Wigner law. In this framework, we also showed that the difference in the localization patterns between fast-decaying left and right eigenfunctions can be recognized as an artifact, inherent in the construction of open quantum maps.

(iii) Analogous simulations of the discretized classical evolution operator result in a deviation of the intensity distribution from the RMT expectations akin to what is observed in the quantum setting, when the coupling to the opening is weak enough for perturbation theory to be valid. A stronger coupling to the opening increases the number of fast-decaying states, so as to obtain a longer-tailed intensity distribution, very different from the resonance trapping observed in the quantum simulations.

ACKNOWLEDGMENTS

This research was supported by the Basic Science Research Program through the National Research Foundation of Korea (NRF) funded by the Ministry of Science, ICT, and Future Planning (2013R1A1A2011438). D.L. acknowledges support from the National Science Foundation of China (NSFC), International Young Scientists (11450110057-041323001).

APPENDIX: DERIVATION OF EQ. (4)

We start from the joint probability distribution [30] of $\eta = \sum_{p\neq n} \frac{|\xi|^2}{E_n - E_p}$ and $\zeta = \sum_{p\neq n} \frac{|\xi|^2}{(E_n - E_p)^2}$,

$$P(\eta,\zeta) \propto \frac{(1+\gamma^2\eta^2)^M}{\zeta^{2+3M/2}} e^{-\frac{M\pi}{2\gamma\zeta}(1+\gamma^2\eta^2)}, \tag{A1}$$

with M number of degrees of freedom. We simply integrate over ζ to obtain the distribution of η, in one [Eq. (4)] or M [Eq. (31)] degrees of freedom.

[1] J. P. Eckmann and D. Ruelle, Rev. Mod. Phys. **57**, 617 (1985).
[2] M. V. Berry and M. Tabor, Proc. R. Soc. London, Ser. A **356**, 375 (1977).
[3] H. J. Stöckmann, *Quantum Chaos: An Introduction* (Cambridge University Press, Cambridge, 1999).
[4] E. P. Wigner, *Group Theory and Its Application to the Quantum Mechanics of the Atomic Spectra* (Academic, New York, 1959).
[5] M. L. Mehta, *Random Matrices* (Elsevier, Amsterdam, 2006).
[6] T. Prosen, T. Seligman, and M. Žnidarič, Prog. Theor. Phys. Suppl. **150**, 200 (2003); T. Prosen and M. Žnidarič, J. Phys. A **34**, L681 (2001).
[7] B. Georgeot and D. L. Shepelyansky, Phys. Rev. Lett. **86**, 2890 (2001).
[8] W. H. Zurek, Rev. Mod. Phys. **75**, 715 (2003).
[9] J. U. Nöckel and A. D. Stone, Nature (London) **385**, 45 (1997).
[10] M. Hentschel and K. Richter, Phys. Rev. E **66**, 056207 (2002).
[11] J. R. Ackerhalt, P. W. Milonni, and M.-L. Shih, Phys. Rep. **128**, 205 (1985).
[12] C. Emary and T. Brandes, Phys. Rev. Lett. **90**, 044101 (2003).
[13] F. L. Moore, J. C. Robinson, C. Bharucha, P. E. Williams, and M. G. Raizen, Phys. Rev. Lett. **73**, 2974 (1994); F. L. Moore, J. C. Robinson, C. F. Bharucha, B. Sundaram, and M. G. Raizen, *ibid.* **75**, 4598 (1995).
[14] C. W. J. Beenakker, Rev. Mod. Phys. **69**, 731 (1997).
[15] F. Miao, S. Wijeratne, Y. Zhang, U. C. Coskun, W. Bao, and C. N. Lau, Science **317**, 1530 (2007).
[16] T. A. Brun, I. C. Percival, and R. Schack, J. Phys. A **29**, 2077 (1996).
[17] S. Nonnenmacher, Nonlinearity **24**, R123 (2011).
[18] L. Kaplan, Phys. Rev. E **59**, 5325 (1999).
[19] H. P. Breuer and F. Petruccione, *The Theory of Open Quantum Systems* (Oxford University Press, Oxford, 2002).
[20] R. Pnini and B. Shapiro, Phys. Rev. E **54**, R1032 (1996).
[21] P. Seba, F. Haake, M. Kus, M. Barth, U. Kuhl, and H.-J. Stöckmann, Phys. Rev. E **56**, 2680 (1997).
[22] H. Ishio, A. I. Saichev, A. F. Sadreev, and K.-F. Berggren, Phys. Rev. E **64**, 056208 (2001).
[23] E. J. Heller, Phys. Rev. Lett. **53**, 1515 (1984).
[24] L. Kaplan and E. J. Heller, Ann. Phys. (N.Y.) **264**, 171 (1998).
[25] L. Kaplan, Phys. Rev. Lett. **80**, 2582 (1998).
[26] I. Rotter, Rep. Prog. Phys. **54**, 635 (1991).
[27] V. V. Sokolov and V. G. Zelevinsky, Nucl. Phys. A **504**, 562 (1989).

[28] P. Cvitanović, R. Artuso, R. Mainieri, G. Tanner, and G. Vattay, *Chaos: Classical and Quantum*, ChaosBook.org (Niels Bohr Institute, Copenhagen, 2009).
[29] S. C. Creagh, Chaos **5**, 477 (1995).
[30] H. Schomerus, K. M. Frahm, M. Patra, and C. W. J. Beennakker, Physica A **278**, 469 (2000).
[31] C. Poli, D. V. Savin, O. Legrand, and F. Mortessagne, Phys. Rev. E **80**, 046203 (2009).
[32] C. Poli, O. Legrand, and F. Mortessagne, Phys. Rev. E **82**, 055201(R) (2010).
[33] Y. V. Fyodorov and D. V. Savin, Phys. Rev. Lett. **108**, 184101 (2012).
[34] S. C. Creagh, S. Y. Lee, and N. D. Whelan, Ann. Phys. (N.Y.) **295**, 194 (2002).
[35] J. H. Hannay and M. V. Berry, Physica D **1**, 267 (1980).
[36] J. P. Keating and F. Mezzadri, Nonlinearity **13**, 747 (2000).
[37] D. Lippolis, J.-W. Ryu, S.-Y. Lee, and S. W. Kim, Phys. Rev. E **86**, 066213 (2012).
[38] P. Kleinwächter and I. Rotter, Phys. Rev. C **32**, 1742 (1985).
[39] F.-M. Dittes, H. L. Harney, and I. Rotter, Phys. Lett. A **153**, 451 (1991).
[40] I. Rotter, E. Persson, K. Pichugin, and P. Seba, Phys. Rev. E **62**, 450 (2000).
[41] E. Persson and I. Rotter, Phys. Rev. C **59**, 164 (1999).
[42] F. M. Izrailev, D. Saher, and V. V. Sokolov, Phys. Rev. E **49**, 130 (1994).
[43] I. Rotter, Phys. Rev. E **64**, 036213 (2001).
[44] H.-J. Stöckmann, E. Persson, Y. H. Kim, M. Barth, U. Kuhl, and I. Rotter, Phys. Rev. E **65**, 066211 (2002).
[45] H. Schomerus and J. Tworzydlo, Phys. Rev. Lett. **93**, 154102 (2004).
[46] Y. V. Fyodorov and H.-J. Sommers, JETP Lett. **72**, 422 (2000).
[47] J. J. Sakurai, *Modern Quantum Mechanics* (Addison-Wesley, Reading, MA, 2011).
[48] H. Goldstein, C. Poole, and J. Safko, *Classical Mechanics* (Addison-Wesley, Reading, MA, 2002).
[49] P. Gaspard, *Chaos, Scattering, and Statistical Mechanics* (Cambridge University Press, Cambridge, 1999).
[50] P. Gaspard, G. Nicolis, A. Provata, and S. Tasaki, Phys. Rev. E **51**, 74 (1995).
[51] H. Risken, *The Fokker-Planck Equation* (Springer-Verlag, Berlin, 1996).
[52] S. Fishman, in *Supersymmetry and Trace Formulae: Chaos and Disorder*, edited by I. V. Lerner, J. P. Keating, and D. E. Khmelnitskii (Springer, New York, 1999), pp. 193–226.
[53] M. Khodas, S. Fishman, and O. Agam, Phys. Rev. E **62**, 4769 (2000).
[54] K. Pance, W. Lu, and S. Sridhar, Phys. Rev. Lett. **85**, 2737 (2000).
[55] S. M. Ulam, *A Collection of Mathematical Problems* (Interscience, New York, 1960).
[56] L. Ermann and D. L. Shepeliansky, Eur. Phys. J. B **75**, 299 (2010).